Metallophysics and Advanced Technologies
Металофіз. новітні технол.
Metallofiz. Noveishie Tekhnol.
2024, vol. 46, No. 5, pp. 431–452
https://doi.org/10.15407/mfint.46.05.0431
Reprints available directly from the publisher

PACS numbers: 06.60.Vz, 68.37.Yz, 78.70.En, 81.20.Vj, 81.40.Ef, 81.40.Lm, 81.70.Bt

Study on Normalizing and Tempering Treatment Regime of Homogenization of P92 Weldments

V. K. Pal and L. P. Singh

Department of Mechanical Engineering,
Sam Higginbottom University of Agriculture, Technology and Sciences Allahabad,
IN-211007 Uttar Pradesh, India

The present research work describes the effect of normalizing and tempering (N&T) treatment on microstructure evolution in various zones of gas tungsten arc-welded (GTAW) P92 pipe weldments. For N&T treatment, P92 pipe weldments are subjected to various normalizing (950–1150°C) and tempering (730–800°C) temperatures. The effect of varying heat treatment on tensile properties and hardness of P92 pipe weldments are studied for V-groove and narrow-groove weld designs. The effect of increase in normalizing temperature (at fixed tempering temperature) results in increase in strength and hardness, while increase in tempering temperature (at fixed normalizing temperature) results in the decrease in strength and hardness of P92 steel weldments. Creep strength-enhanced ferritic/martensitic P92 steel is considered as a candidate material for the reactor pressure vessels and reactor internals of Very High Temperature Reactor (VHTR). The heterogeneous microstructure formation across the P92 weldments leads to premature Type IV cracking and makes the weldability of P92 steel as a serious issue. The better combination of strength, ductility and microstructure are obtained for the maximum normalizing temperature of 1050°C and tempering temperature of 760°C. The effect of increase in normalizing temperature (at fixed tempering temperature) results in increase in strength and hardness, while increase in tempering temperature (at fixed normalizing temperature) results in the decrease in strength and hardness of P92 steel weldments.

Key words: normalizing, tempering, P92 pipe weldments, microstructure, mechanical properties.

Corresponding author: Vinay Kumar Pal
E-mail: gaurishankar.vinaypal@gmail.com

Citation: V. K. Pal and L. P. Singh, Study on Normalizing and Tempering Treatment Regime of Homogenization of P92 Weldments, *Metallofiz. Noveishie Tekhnol.*, **46**, No. 5: 431–452 (2024). DOI: 10.15407/mfint.46.05.0431

У цій дослідницькій роботі описано вплив нормалізації та відпуску на еволюцію мікроструктури в різних зонах зварних з'єднань труб P92, зварених газовольфрамовим дуговим зварюванням. Для нормалізації та відпуску зварні з'єднання труб P92 піддавали різним температурам нормалізації (950–1150°C) та відпуску (730–800°C). Вплив різного термічного оброблення на розривні властивості та твердість зварних швів труб P92 вивчали для V-подібних і вузькоканавочних зварних швів. Підвищення температури нормалізації (за фіксованої температури відпуску) привело до збільшення міцности та твердости, тоді як пониження температури відпуску (за фіксованої температури нормалізації) призвело до зменшення міцности та твердости зварних з'єднань із криці P92. Феритно-мартенситна криця P92 з підвищеною міцністю на плазучість розглядається як матеріял-кандидат для корпусів реактора та внутрішніх частин надвисокотемпературного реактора (HBTP). Неоднорідна мікроструктура, що утворюється у зварних швах із криці P92, призводить до передчасного розтріскування IV типу та робить зварюваність криці P92 серйозною проблемою. Найліпше поєднання міцности, пластичности та мікроструктури було одержано за максимальної температури нормалізації у 1050°C та температури відпуску у 760°C. Ефект підвищення температури нормалізації (за фіксованої температури відпуску) призвів до збільшення міцности та твердости, тоді як підвищення температури відпуску (за фіксованої температури нормалізації) призвело до зменшення міцности та твердости зварних з'єднань із криці P92.

Ключові слова: нормалізація, відпуск, P92-трубні зварні вироби, мікроструктура, механічні властивості.

(Received 7 August 2023; in final version, 5 October 2023)

1. INTRODUCTION

P92 steel processed tempered martensitic microstructure obtained by normalizing and tempering treatment (N&T). Normalizing of P91 steel is generally carried out in the austenitizing temperature range of 1040–1060°C for 20–40 min, followed by air-cooling. The subsequent tempering is performed in the temperature range of 730–780°C for 1–2 h, followed by air-cooling. The strength of P92 steel is primarily derived from its stable microstructure. The stability of microstructure is governed by the tempered martensitic lath structure, sub-grain size, prior-austenite grain boundaries (PAGBs), lath width, lath boundaries, precipitate size and their distribution inside the structure, dislocation density, precipitate morphology and their amount [1]. Very High Temperature Reactor (VHTR), Sodium cooled fast reactors (SFRs) are being developed to fulfil the growing energy demand with a view to greater reliability, safety, economy and lesser environmental pollution [2, 3]. 9% Cr CSEF/M steels development started from last few decades, starting from plain 9Cr–1Mo (P9), modified 9Cr–1Mo

(P91) and P92 steel. P91 steel is next version of plain 9Cr–1Mo steel, which was developed in Oak-Ridge National Laboratory (ORNL) by modifying the chemical composition of P9 steel [4, 5]. P92 steel was developed by adding the strong carbide and carbonitride former element such as 0.2 wt.% vanadium, 0.08 wt.% niobium, and 0.05 wt.% nitrogen. El-Azim *et al.* [6] performed a comparative study on creep behaviour of P91 steel joint and base metal. The creep strength of base metal was observed to be superior to weld joint at higher creep exposure temperature about 650°C while at a lower temperature about 600°C, it approached to creep strength of the base metal. Fracture location was observed in the base metal near to HAZ for short-term creep exposure (426 h) at 600°C and high applied stress of 150 MPa. The lower applied stress for same applied temperature was resulted in shifting of fracture location and type IV fracture occurred in FGHAZ of the weld joint. Laha *et al.* [7] reported the soft zone formation in IC-HAZ of P91 joint and type IV fracture was associated with IC-HAZ. Maruyama *et al.* [8] reported that the precipitate remains undissolved are mainly Type I Nb*X*. The undissolved precipitates limit the austenitic grain growth during normalizing treatment. The undissolved MX precipitates provide the pinning effect to grain boundaries and produce a fine-grained structure during normalizing. The modified *Z*-phase comes out after long-term exposure at a temperature about 600–700°C [9]. The dissolution temperature of modified *Z*-phase was reported about 800°C which is much lower than the solution temperature of original *Z*-phase (1200–1250°C) [9]. The heating of creep exposure steel above 800°C resulted in the formation of M*X* nitride from the *Z*-phase [10]. Abd El-Salam *et al.* [11] had incorporated the effect of normalizing/tempering (N&T) treatment on microstructure homogenization of shielded metal arc welded P91 joint and compared it with subsequent PWHT. For N&T treatment, the optimum degree of hominization was observed along the weldments that were attributed due to the recrystallization effect during the normalizing. Manugula *et al.* [12] had performed the N&T and subsequent PWHT for electron-beam welded reduced activated ferritic–martensitic steel. The weld was produced with poor toughness and high hardness due to the presence of δ-ferrite in the martensitic microstructure. Subsequent PWHT resulted in significant reduction in hardness of weld fusion zone but the heterogeneous distribution of hardness across the weldments was still present with δ-ferrite. Albert *et al.* [13] have also studied the effect of PWHT duration on type IV cracking nature in P122 weld joints. The creep test was performed at 650°C for 70 MPa. PWHT duration was varied from 15 min to 4 h, but no any significant change was observed in creep rupture time and fracture behaviour. In all the cases, type IV fracture was observed. Sawada *et al.* [14] have studied the cross-weld long-term creep behaviour of E911 joint at 600°C. The fracture was noticed in

soft FGHAZ. The growth of $M_{23}C_6$ in FGHAZ was observed faster than the base metal. The *Z*-phase formation was observed both in FGHAZ and base metal FGHAZ exhibited higher number density of *Z*-phase than the base metal. For long-term creep exposure at the low level of stress, creep life was observed to be minimum in FGHAZ [15].

A systematic study of different normalizing and tempering temperature combination that leads to the optimum combination of mechanical properties and microstructure stability, considering the necessity of effect of N&T treatment on microstructure stability and mechanical properties of P92 steel weldments, efforts are being made to perform.

2. EXPERIMENTAL DETAILS

2.1. Groove Design and Welding Process Parameters

The base metal used for the experiment was P92 pipe with an outer diameter of 60.3 mm and thickness of 11 mm. Gas tungsten arc welding (GTAW) of P92 pipes was carried out using conventional V-groove and narrow-groove designs. The conventional V-groove and narrow grove pipes and weld design is shown in Fig. 1, *a*–*c*. The conventional V-groove design used for the weld confirms to Section IX of the ASME Boiler and Pressure Vessel Code. Initial groove openings for conventional V-groove and narrow-groove were 14.58 and 9.06 mm, respectively (as measured after groove preparation). The conventional V-grooved and narrow-grooved pipes after the tack welding are shown in Fig. 2, *a*. To weld the P92 pipe joints using the GTAW process, a welding turntable with a rotating three-jaw self-centring chuck was uti-

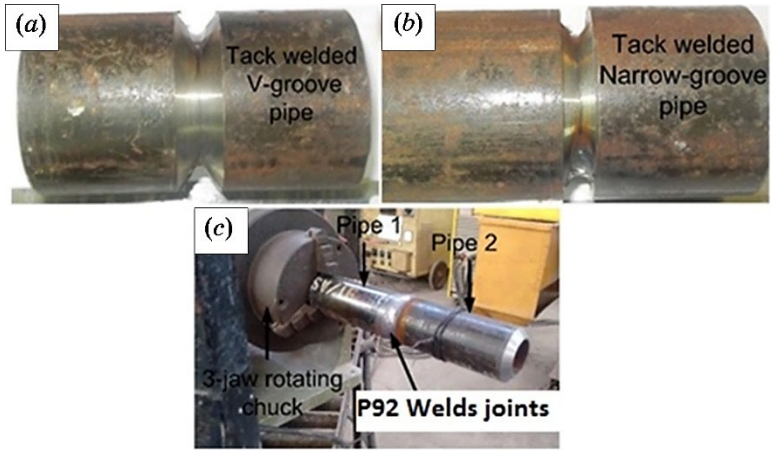

Fig. 1. (*a*) and (*b*) grooved pipe joints with tacking, (*c*) experimental set-up with welded pipe joints.

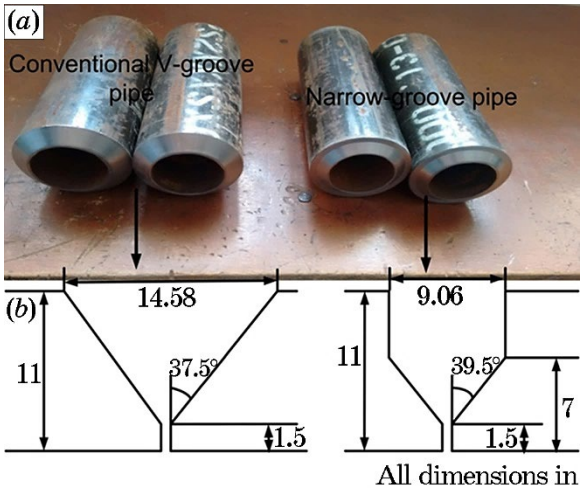

Fig. 2. (*a*) P92 pipe with conventional and narrow weld-groove design (*b*) Conventional V-groove and narrow-groove design.

TABLE 1. Chemical composition of P92 pipe, AWSER90S-B9 (9CrMoV-N) filler wire, and weld metal (wt.%).

Element	C	Mn	Cr	Si	Mo	V	Nb	Ni	S	Ti	W	Cu	Fe
P92 steel	0.12	0.54	8.48	0.28	0.95	0.18	0.05	0.35	0.011	0.012	<0.001	0.06	Rest
Filler metal	0.12	0.50	8.83	0.30	0.90	0.20	0.06	0.50	0.019	0.001	–	–	Rest
Weld metal	0.11	0.52	8.28	0.28	0.87	0.20	0.04	0.44	0.019	<0.002	<0.001	0.05	Rest

lized. P92 pipes of 150 mm length were multipass welded (eight passes for conventional V-groove and seven passes for narrow-groove) at 1-GR position (pipe rolled in flat position), as shown in Fig. 2, *b*. The welded pipe joints with experimental set-up are shown in Fig. 2, *b*.

The AWSER90S-B9 (9CrMoV–N) filler wire with a diameter of 1.6 mm was used for the GTAW purpose. The composition of the as-received material, filler wire and weld metal are given in Table 1. GTAW parameters for the root pass were 110 A DC and 12 V. For subsequent GTAW passes, the filling parameters are given in Table 2. To maintain the linear travel speed of 2.11 mm/s during the filling pass, a motor-controlled fixture was used. The preheat temperature of 250°C was maintained by using the flame heating and interpass temperature was selected in the range of 200–250°C. For the shielding purpose,

TABLE 2. Welding process parameter.

Nos. of passes	Current (amp)	Voltage (V)	Travel speed (mm/sec)	Current (amp)	Voltage (V)	Travel speed (mm/sec)
	Conventional V-groove			Narrow-groove		
Root pass	105–115	12	1.47	105–115	12	1.47
1	110–115	12–14	2.11	110–115	12–15	2.11
2	120–125	12–15	2.11	110–115	12–15	2.11
3	118–124	14–16	2.11	112–120	14–16	2.11
4	120–123	12–14	2.11	118–124	15–18	2.11
5	110–115	18–20	2.11	118–124	14–18	2.11
6	112–120	14–16	2.11	115–120	14–15	2.11
7	120–125	12–14	2.11	114–118	13–16	2.11
8	120–125	12–15	2.11	–	–	–

pure argon gas was used with a flow rate of 15 l/min.

2.2. Heat Treatment of P92 Weldments

After the completion of welding, the weld joints were subjected to three different heat conditions as per given Table 3 One welded pipe joint of each groove type (V-groove and narrow groove) was allowed to cool in air up to room temperature without any heat treatment. The second one from each groove design was subjected to post-weld heating before post weld heat treatment (PWHT). Generally, post-weld heating of P92 weld to 250–300°C for 30 to 60 min followed by air cooling up to 100°C is recommended before PWHT for removing the diffusible hydrogen. The cooling is carried out to ensure the formation of complete martensitic microstructure just before PWHT, as residual austenite does not respond to the PWHT, which leads to the formation of harmful untempered martensite [16]. After the post-weld heating, subsequent PWHT was performed at 760°C for 2 h. The third weld joint was subjected to conventional normalizing and tempering or post weld normalizing and tempering (PWNT) heat treatment. The weld joints were reaustenitized at 1050°C for 40 min and air cooled, then tempered at 760°C for 2 h, and finally air-cooled. The PWHT was performed to homogenize the microstructure and remove the quench stresses by tempering the lath martensite. The PWHT temperature range should be below than the critical temperature (A_{c1}), which mainly depends on the fusion zone composition (Ni + Mn content). Newell [17] had also

TABLE 3. Different heat treatment condition performed just after the welding for V-groove and narrow groove designs.

P92 pipe weldments	Heat treatment condition
1 (as-welded)	After welding, allowed to cool in air up to room temperature
2 (PWHT)	After welding, PWHT in range of 250–300°C for 30 to 60 min and then air cooling up to 100°C followed by PWHT at 760°C for 2 h, followed by air cooling
3 (PWNT)	After welding, normalized at 1040°C for 60 min, and air-cooled and tempered at 760°C for 2 h, followed by air cooling

suggested that for the large size specimens, the PWHT temperature should be lower than A_{c1} by 10 to 20°C. Based on the Ni + Mn content in weld fusion zone, Santella *et al.* [18] had proposed a mathematical equation to calculate the A_{c1} temperature.

The equation is given below:

$$A_{c1}\,(°C) = 854{\cdot}5 \pm 0.6 - 43{\cdot}9 \pm 1 \times (Mn + Ni) - 9 \pm 0.4 \times (Mn + Ni)^2. \quad (1)$$

From this equation and Table 1, the A_{c1} temperature was calculated about 809°C. The PWHT parameter was as per the code recommended following ASME B31.1—760°C for 2 h.

2.3. Mechanical Testing and Characterization

To study the effect of different heat treatments (as-welded and PWHT) on yield strength, ultimate tensile strength, and percentage elongation of P92 steel weld joints, flat tensile test specimen was prepared as per ASTM A370-14 [19]. The room temperature tensile tests were performed on the vertical tensile testing specimen (Instron: 5982) at the constant crosshead speed of 1 mm/min. The gauge length and width of the flat tensile specimen were 50 mm and 11.8 mm, respectively. The microhardness of welded samples before and after PWHT was measured by using a Vickers hardness tester at a load of 500 g and dwell time of 10 s. Cross-sectional samples were prepared from welded pipes for both the conventional and narrow-groove designs in order to measure the hardness in various weld zones and base metal. The through-thickness hardness at the centre of the weld fusion zone was measured. Furthermore, the hardness was also measured across the welds at 4 mm below the weld reinforcement outer surface.

For both the through the thickness and across the weld hardness measurements, indented points were located along a straight line at

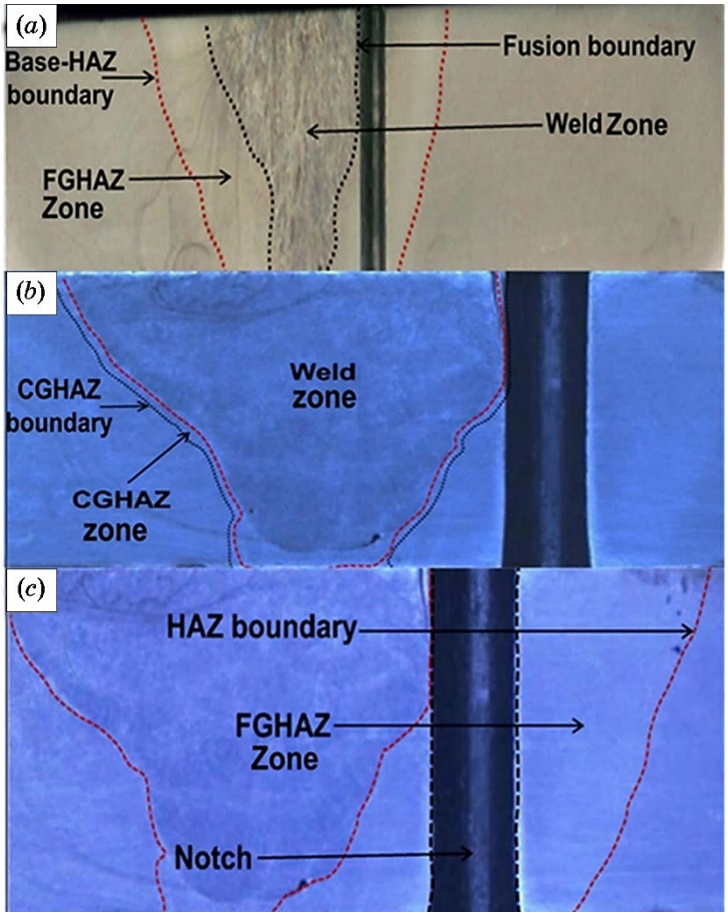

Fig. 3. Macrostructure of impact toughness specimens showing (*a*) weld zone, FGHAZ zone, base-HAZ boundary, fusion zone boundary, (*b*) CGHAZ boundary and CGHAZ zone, and (*c*) a notch adjacent to fusion boundary.

1 mm intervals. To study the impact toughness of P92 base metal in different operating temperature conditions, flat samples of 7.5 mm thickness were prepared from the pipe. Standard sub-size Charpy impact V-notch specimens ($55\times10\times7.5$ mm^3) were prepared according to ASTM A370-14 [19]. Charpy toughness tests were performed in the temperature range of 25–1000°C. For each test, three samples were prepared and an average of three test results has been reported.

To study the Charpy toughness of HAZ, notches were prepared in the HAZ of both conventional V-groove and narrow-groove-welded joints. Weld samples were polished using emery paper up to grit size 600 and then etched with Nital solution (10% nitric acid in methanol) to reveal the fusion boundary, which served as the location for prepa-

TABLE 4. Different operating condition to evaluate the impact toughness of HAZ of P92 steel weldment.

S. No.	Conventional V-groove	Narrow groove
1	Charpy test at room temperature	Charpy test at room temperature
2	Hot Charpy test at 760°C	Hot Charpy test at 760°C
3	Charpy test at room temperature after PWHT at 760°C for 2 h	Charpy test at room temperature after PWHT at 760°C for 2 h
4	Hot Charpy test at 760°C after PWHT at 760°C for 2 h	Hot Charpy test at 760°C after PWHT at 760°C for 2 h

ration of notches as shown in Fig. 3. The different operating conditions considered for Charpy toughness testing of HAZ of P92 steel weldments are stated in Table 4. Charpy toughness tests were also conducted to study the effect of post-weld heating at 280°C for 40 min and 60 min just after welding on the impact toughness of P91 weld fusion zone and HAZ. To study the effect of subsequent PWHT and PWNT heat treatment on tensile properties of different weld groove designs, round subsize tensile-test specimens were prepared as per to ASTM E8-E8M-13a [20] standards with a gauge diameter of 6 mm.

3. RESULTS

3.1. As-Received Materials and Microstructure

The microstructure of weld fusion zone and FGHAZ in as welded condition are presented in Fig. 4, *a*, *b*. The weld fusion zone is characterized with columnar laths in packets form with similar spatial orientation inside the PAGBs with almost negligible precipitates, as shown in Fig. 4, *a*. The precipitates are dissolved at such high temperature and increase the carbon (C) percentage in martensite that makes it brittle with high strength and poor toughness. The heterogeneous microstructure mainly occurred among weld fusion zone, ICHAZ and FGHAZ. In P92 weldments, it is quite difficult to distinguish the FGHAZ and IC-HAZ. The most common type IV failure of P92 weldments are initiated from FGHAZ or IC-HAZ because of soft zone (low hardness). The FGHAZ are partially austenitized during weld thermal cycle because of low temperature as compared to weld fusion zone and CGHAZ. FGHAZ shows a complex structure of newly formed grain and existing grains with coarse undissolved $M_{23}C_6$ precipitates, as shown in Fig. 4, *b*.

After the PWHT, secondary electron micrograph of weld fusion zone and FGHAZ are shown in Fig. 4, *c*, *d*.

In weld fusion zone, a number of particles re-precipitated along the boundaries and inside the matrix region. The columnar laths mainly braked into equiaxed lath and tempered martensitic microstructure along with precipitates have been observed. The size of lath width was measured in the range of 3.74–4.68 μm, as shown in Fig. 4, *c*. The grain coarsening was clearly noticed in the FGHAZ after the PWHT. After

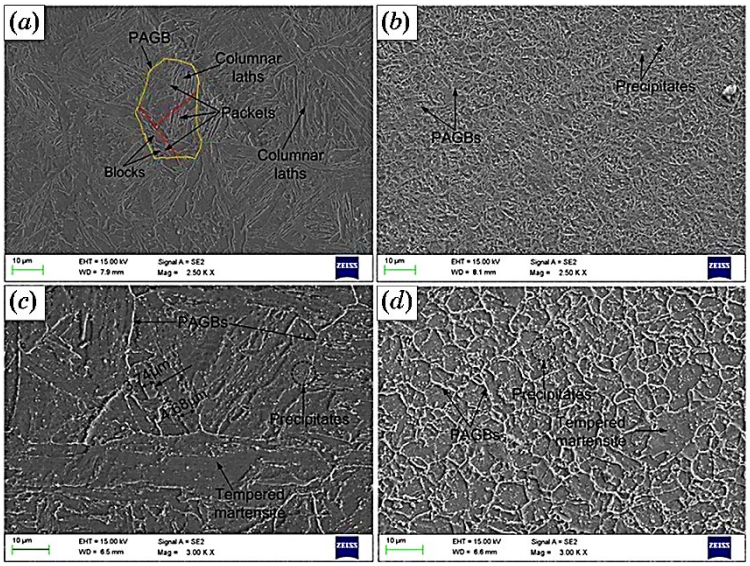

Fig. 4. Microstructure of weld fusion zone and FGHAZ in as-welded condition (*a*) and (*b*); microstructure after the PWHT for weld fusion zone and FAHAZ (*c*) and (*d*).

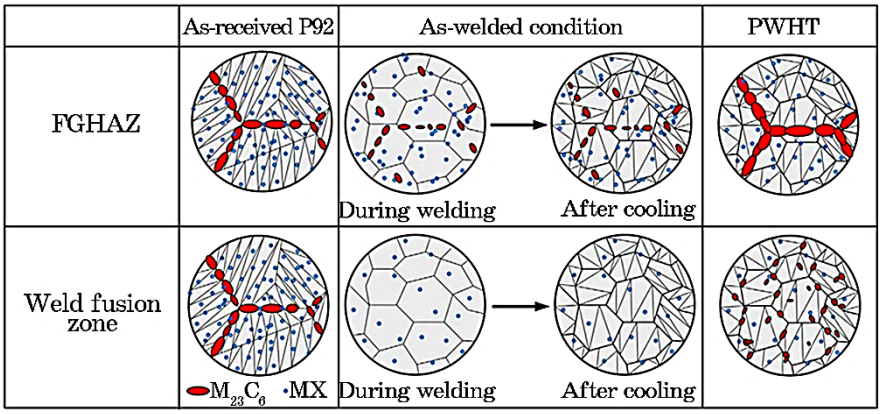

Fig. 5. Characteristic of microstructure in weld zone and FGHAZ in as-welded and PWHT condition.

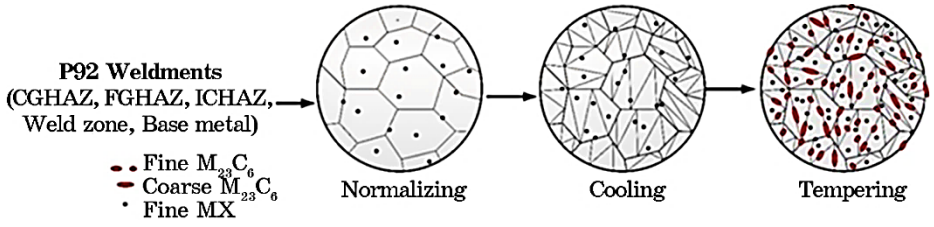

Fig. 6. Schematic of microstructure evolution in subzone of P92 weldments during PWNT treatment.

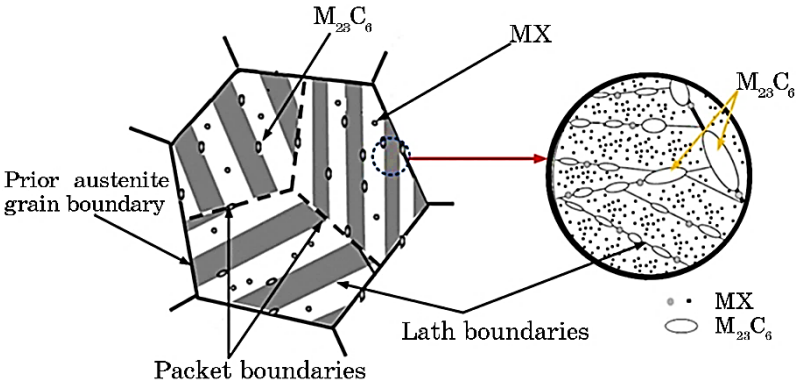

Fig. 7. Schematic evolution of $M_{23}C_6$ and MX precipitates.

PWHT, coarse undissolved $M_{23}C_6$ and newly developed fine MX and $M_{23}C_6$ precipitates are observed in FGHAZ. The PWHT results in the tempered martensitic structure formation with coarse and fine precipitates along the boundaries and grain interior region.

The schematic diagram showing the microstructure evolution in as-welded and PWHT state of weld fusion zone and FGHAZ is depicted in Fig. 5.

After the study of the effect of PWHT, an attempt has been made to perform a comparative study between subsequent PWHT and PWNT heat treatment. In normalizing condition, various zones can be treated as the normalized base metal. Tempering after the normalizing results in the evolution of precipitates along the PAGBs, lath boundaries, packets and inside the intralath region. The subzone of P92 weldments can be treated as the virgin P92 steel.

Schematic of PWNT treatment process and their effect on microstructure evolution is shown in Fig. 6. The study was related to the effect of PWNT heat treatment on microstructure evolution, residual hardness, Charpy toughness and tensile properties of P92 weldment and these results were compared to that of subcritical PWHT.

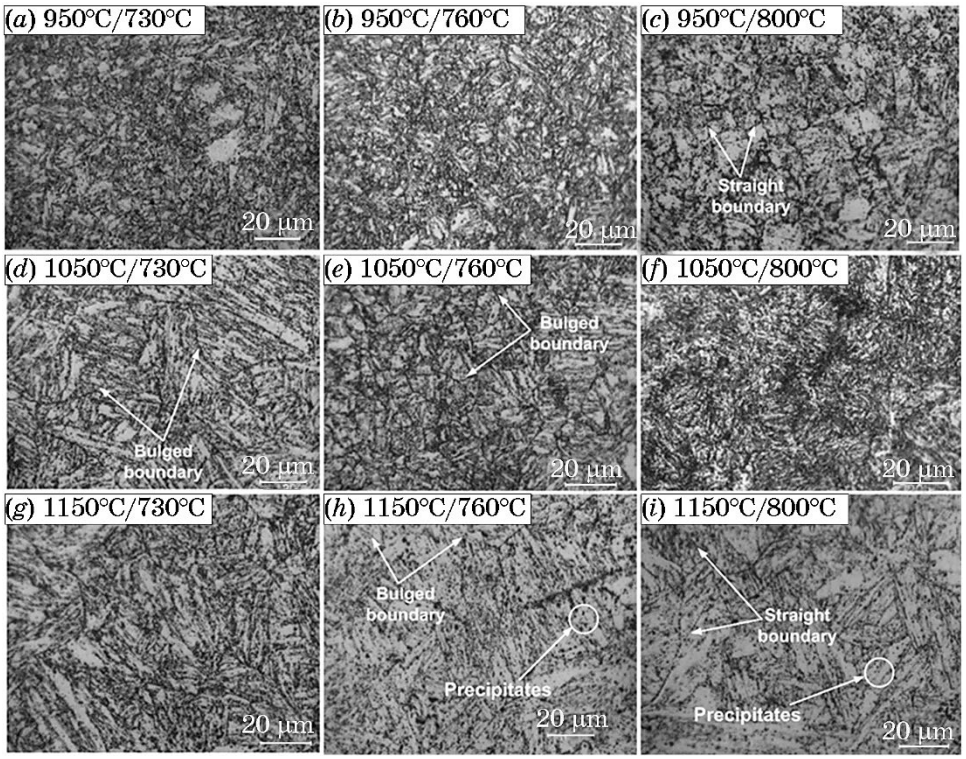

Fig. 8. Optical micrographs of weld fusion zone for different normalized and tempered conditions (*a*) 950°C/730°C, (*b*) 950°C/760°C, (*c*) 950°C/800°C, (*d*) 1050°C/730°C, (*e*) 1050°C/760°C, (*f*) 1050°C/800°C, (*g*) 1150°C/730°C, (*h*) 1150°C/760°C, (*i*) 1150°C/800°C.

Figure 7 shows the schematic diagram of PAGBs, lath boundaries, packet boundaries, lath blocks and precipitates evolution along the boundaries and lath blocks. From Fig. 7, it is clear that the coarse $M_{23}C_6$ precipitates are formed along the PAGBS and lath boundaries while MX precipitates inside the intra-lath region. Hence, area fraction of precipitates mainly depends on the availability of grain boundaries in the microstructure.

3.2. Microstructure Evolution in Weld Zone and FGHAZ for Varying PWNT Conditions

The microstructure of weld fusion zone for different normalized and tempered condition is depicted in Fig. 8, *a*–*i*. The bulged grain boundary at low tempering temperature and straight boundary at higher tempering temperature are shown in Fig. 8, *h* and Fig. 8, *i*. For higher

normalizing and lower tempering temperature, less fraction area of precipitates makes the grain boundaries free from pinning effect that resulted in bulging of the grain boundary. For lower normalizing and higher tempering temperature, the availability of a large number of grain boundaries led to higher fraction area of precipitates. This results in restriction of grain boundary movement leading to straight boundary formation.

The optical micrographs of the fine-grained heat-affected zone (FGHAZ) are shown in Fig. 9, *a–i*. In FGHAZ, the similar pattern of grain structure was noticed as obtained for the weld fusion zone. The grain size is observed to increase with an increase in normalizing temperature (fixed tempering temperature) and decrease with increase in tempering temperature (fixed normalizing temperature), as shown in Fig. 10, *a*. For a normalizing temperature of 1150°C, bigger size grain boundaries are clearly seen in Fig. 9, *h–i*. The microstructure of FGHAZ is characterized by the presence of tempered martensite,

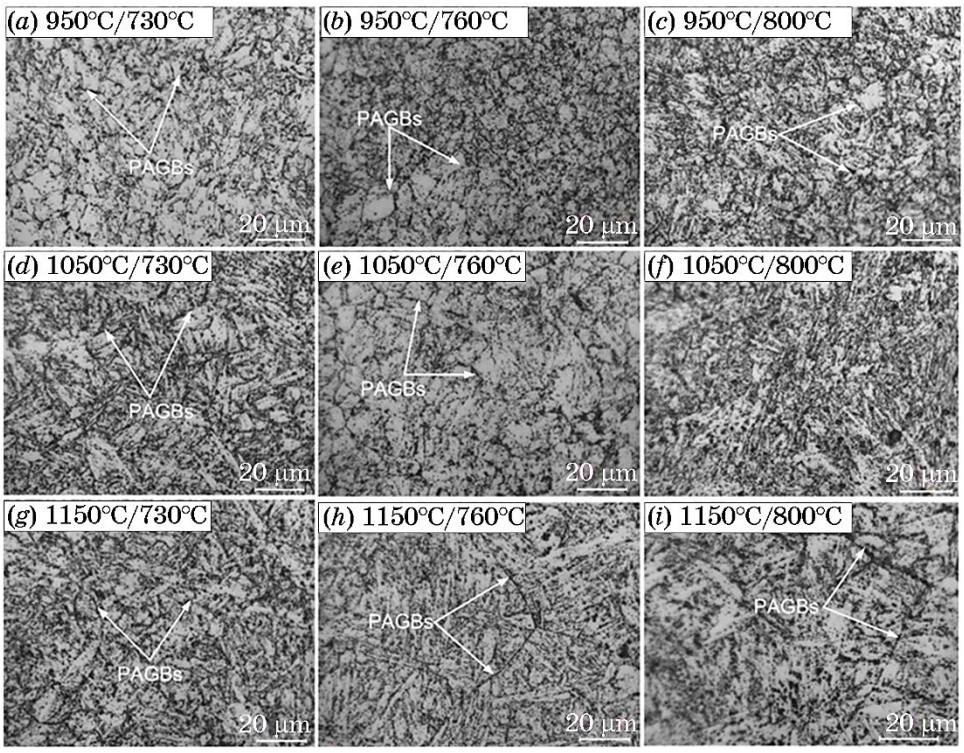

Fig. 9. Optical micrographs of fine-grained heat affected zone for different normalized and tempered conditions (*a*) 950°C/730°C, (*b*) 950°C/760°C, (*c*) 950°C/800°C, (*d*) 1050°C/730°C, (*e*) 1050°C/760°C, (*f*) 1050°C/800°C, (*g*) 1150°C/730°C, (*h*) 1150°C/760°C, (*i*) 1150°C/800°C.

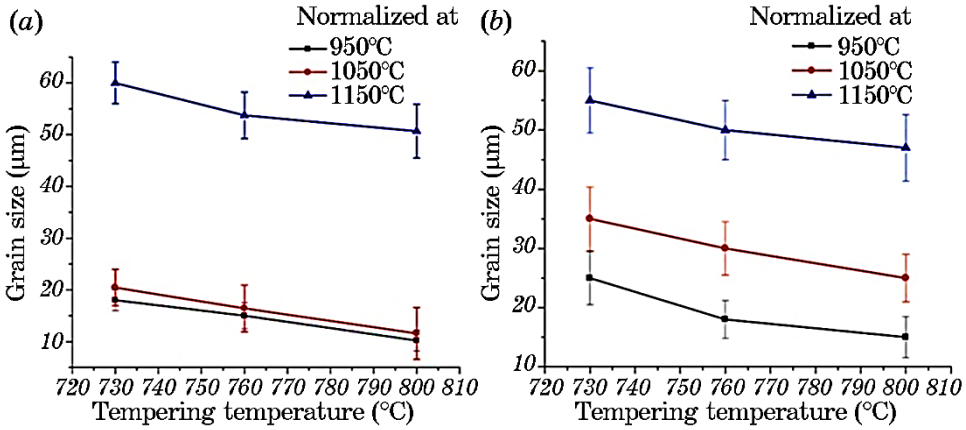

Fig. 10. Variation in grain size with normalizing and tempering temperature (*a*) FGHAZ and (*b*) over-tempered base metal zone.

PAGBs, lath boundaries and packets with $M_{23}C_6$ precipitates along the grain boundaries. The subgrain boundaries are clearly seen in optical micrographs.

The variation in grain size of FGHAZ and over-tempered base zone (OTB) is shown in Fig. 10. For FGHAZ, the grain size increased with an increase in normalizing temperature for a fixed tempering temperature. The grain size decreased with increase in tempering temperature for fixed normalizing temperature. This similar pattern was also observed for the OTB. In FGHAZ, for fixed tempering temperature a negligible change in grain size was observed after increasing the normalizing temperature from 950°C to 1050°C, while a drastic increase was observed after normalizing beyond 1050°C. Grain size plays an important role in determining the strength, hardness and precipitate size distribution. Presence of coarse grain (1150°C/730°C) leads to less availability of grain boundaries, *i.e.*, less fraction area of precipitates. Barbadikar *et al.* [21] had reported that less fraction area of precipitates resulted in the higher availability of C and N in solution matrix that led to solid solution strengthening and ultimately higher strength and hardness.

Secondary electron (SEM) micrograph of weld fusion zones for different normalizing & tempering condition is shown in Fig. 11, *a*–*i*. The distribution of precipitates is clearly seen in SEM micrograph. At low normalizing temperature range (950–1050°C), equiaxed lath morphology is observed while at a higher normalizing temperature of 1150°C lath morphology is observed, and it became difficult to trace the PAGBs. The lath boundaries and packets are clearly seen at a normalizing temperature of 1150°C.

The microstructure of FGHAZ for the different PWNT conditions is

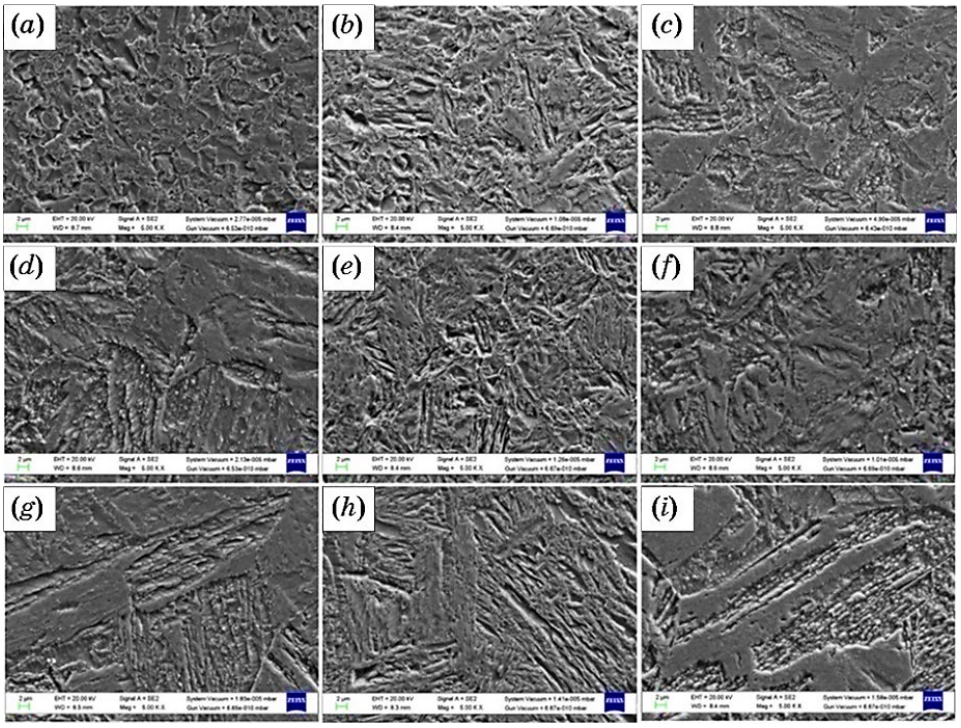

Fig. 11. Secondary electron micrographs of weld fusion zone for different normalized and tempered conditions (*a*) 950°C/730°C, (*b*) 950°C/760°C, (*c*) 950°C/800°C, (*d*) 1050°C/730°C, (*e*) 1050°C/760°C, (*f*) 1050°C/800°C, (*g*) 1150°C/730°C, (*h*) 1150°C/760°C, (*i*) 1150°C/800°C.

shown in Fig. 12, *a–i*. For a low normalizing temperature of 950°C, the microstructure looks similar for each tempering condition except the grain coarsening. For normalizing & tempering of 1050°C/800°C, the microstructure looks different and typical columnar lath morphology is seen, as shown in Fig. 12, *f*. For PWNT of 1150°C/730°C, due to high coarsening rate, the PAGBs disappear and only lath boundaries are observed. With the increase in tempering temperature for a fixed normalizing temperature, continuous reduction in grain size of FGHAZ was predicted (Fig. 10). Due to smaller grain size, the PAGBs are clearly seen in Fig. 12, *a–f*. Initially, the microstructure of weld fusion zone and FGHAZ looks similar up to normalizing & tempering of 1050°C/760°C, after that a drastic change was noticed in the microstructure in terms of PAGBs, lath boundaries and precipitate distribution. At a higher normalizing temperature of 1150°C, columnar lath morphology is clearly seen in micrographs.

The size and distribution of precipitates in FGHAZ were also measured for all the normalizing & tempering conditions, and it is shown in

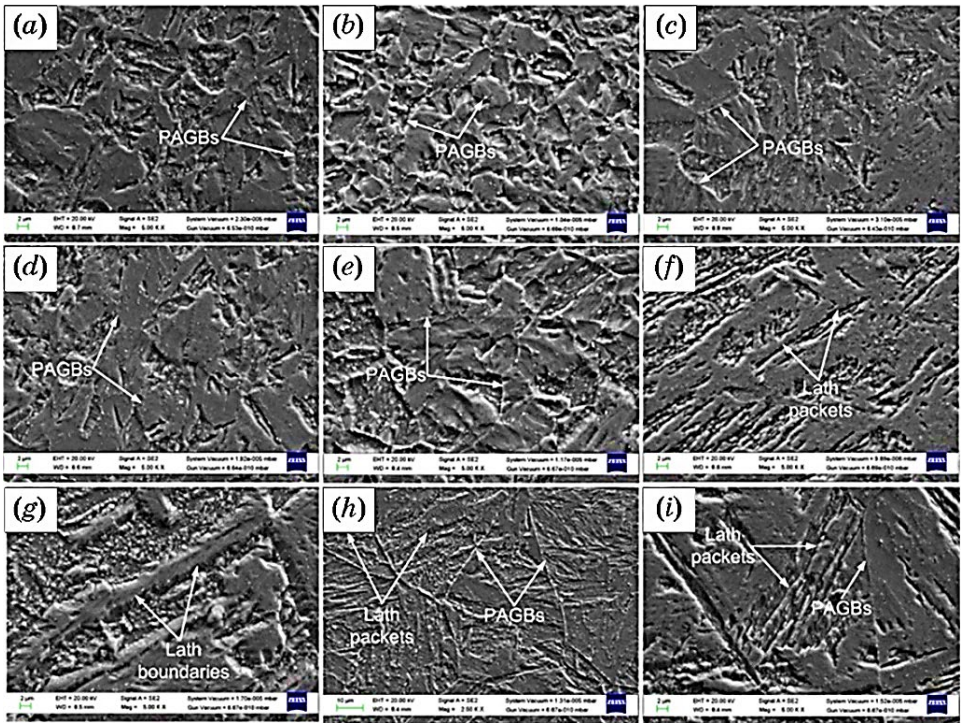

Fig. 12. Secondary electron micrographs of fine-grained heat affected zone for different normalized and tempered conditions (*a*) 950°C/730°C, (*b*) 950°C/760°C, (*c*) 950°C/800°C, (*d*) 1050°C/730°C, (*e*) 1050°C/760°C, (*f*) 1050°C/800°C, (*g*) 1150°C/730°C, (*h*) 1150°C/760°C, (*i*) 1150°C/800°C.

Fig. 13, *a*, *b* for 950°C/730°C and 1150°C/800°C condition. Coarsening of precipitates with an increase in normalizing temperature is clearly noticed in Fig. 13, *a*, *b*. At the initial stage of PWNT process, globular and spherical shape particle are observed, while, at higher PWNT process, mainly cylindrical and needle shaped particles are observed.

The variation in area fraction of precipitates for weld fusion zone and FGHAZ are shown in Fig. 14, *a*, *b*. The area fraction of precipitates increased with increase in tempering temperature (constant normalizing temperature) and decreased with increase in the normalizing temperature (constant tempering temperature) for both weld zone and FGHAZ. The less area fraction of precipitates at low tempering temperature led to the formation of the bulged boundary because of less pinning force from precipitates.

The area fraction of precipitates governs the mechanical properties due to precipitation hardening and solid solution hardening. A higher fraction of precipitates results in a considerable lowering of solid solution hardening due to less availability of C and N in solid solution ma-

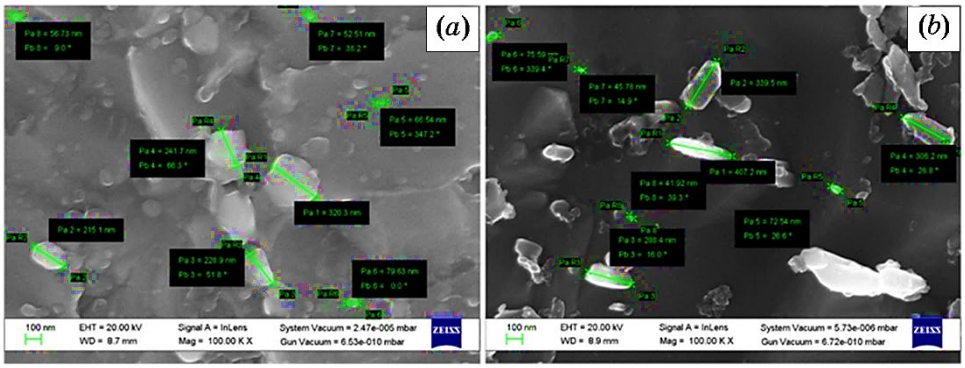

Fig. 13. Size and distribution of element in FGHAZ for different PWNT condition (*a*) 950°C/730°C, (*b*) 1150°C/800°C.

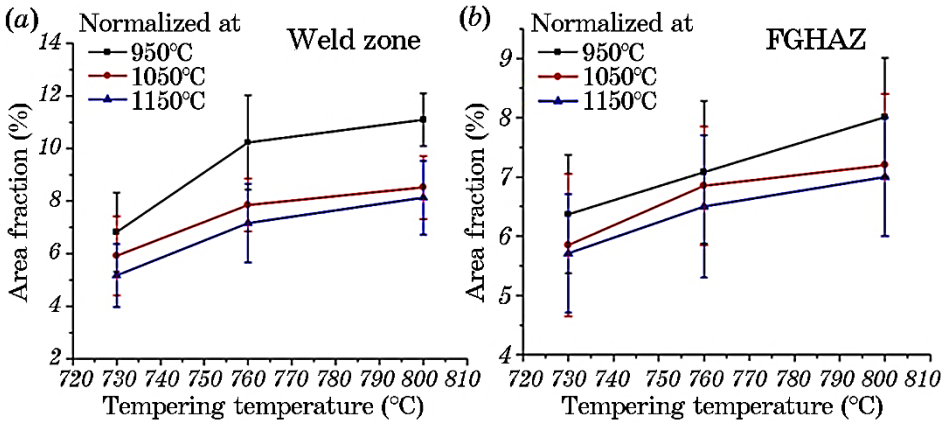

Fig. 14. Variation in area fraction of precipitates (*a*) weld fusion zone and (*b*) FGHAZ.

trix. However, higher fraction area of precipitate might leads to precipitation hardening. Generally, solid solution hardening dominates over the precipitation hardening.

3.3. Hardness Variation

The hardness of weld fusion zone and FGHAZ for different PWNT conditions is given in Table 5. The hardness value increased with increase in normalizing temperature for given tempering temperature while the hardness value decreased with increase in tempering temperature. The extent of increase in hardness in the temperature range of 1050°C–1150°C was found to be more compared to a temperature range

TABLE 5. Hardness variation in weld fusion zone and FGHAZ for different normalizing and tempering condition.

Heat treated condition	Hardness (*HV*)		Heat treated condition	Hardness (*HV*)		Heat treated condition	Hardness (*HV*)	
	Weld zone	FGHAZ		Weld zone	FGHAZ		Weld zone	FGHAZ
950°C/730°C	235 ± 3	235 ± 3	1050°C/730°C	237 ± 2	233 ± 2	1150°C/730°C	238 ± 3	235 ± 3
950°C/760°C	230 ± 3	229 ± 5	1050°C/760°C	232 ± 3	228 ± 4	1150°C/760°C	235 ± 3	231 ± 2
950°C/800°C	232 ± 3	231 ± 3	1050°C/800°C	239 ± 3	233 ± 3	1150°C/800°C	247 ± 2	237 ± 2

of 950°C–1050°. The lower hardness in the temperature range of 950°C–1050°C is attributed to the presence of higher grain boundaries and large fraction area of precipitates. For a normalizing temperature of 1150°C, coarse grain size led to lower precipitation of $M_{23}C_6$ and MX precipitates and ultimately larger presence of carbon and nitrogen in solution matrix that resulted in higher solid solution hardening. Lower precipitate formation resulted in reduced precipitation hardening. Grain coarsening might also lead to poor hardness but higher solid solution hardening dominate over the reduction in precipitation hardening and grain coarsening. This resulted in an increase in hardness value at higher normalizing temperature compared to lower normalizing temperature.

3.4. Tensile Properties

For V-grove and narrow groove weld design, transverse tensile test specimens were tested. The gauge length and width of the flat tensile specimen were 25 mm and 6.25 mm, respectively. For transverse tensile tested specimen, variation in ultimate tensile strength (UTS) and yield strength (YS) with normalizing and tempering are depicted in Fig. 15, *a–d*. In each test, the fracture location was noticed in the OTB. For a fixed tempering temperature, the YS and UTS were increased with an increase in normalizing temperature for both the groove designs. For V-groove design, UTS increased from 705 MPa to 730 MPa with an increase in normalizing temperature from 950°C to 1150°C (tempering temperature 730°C), while, for narrow groove design, it increased from 683 MPa to 712 MPa. The minimum UTS and YS were measured for sample normalized at 950°C and tempered at 800°C for both groove designs. The sample normalized at 1150°C led to coarse grain and higher lath width. This resulted in less availability of grains

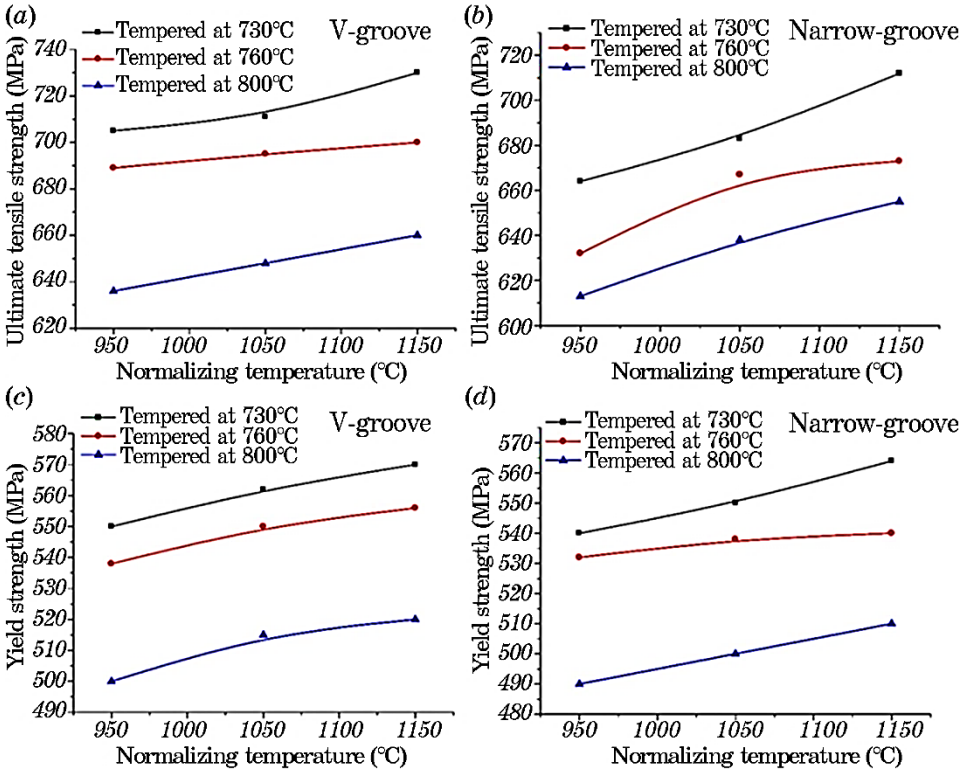

Fig. 15. Variation in tensile properties for V-groove and narrow-groove design with varying normalizing and tempering temperature: (*a*), (*b*) UTS; (*c*), (*d*) YS.

and grain boundaries per unit area and reduced the fraction area of precipitates. The lower availability of carbide precipitates led to solid solution strengthening and resulting in an increase in strength of steel for sample normalized at 1150°C compared to the sample normalized at 950°C and 1050°C. For narrow groove design, similar behaviour was noticed in UTS and YS variation. However, the UTS and YS measured for the narrow groove weld design was found to be less corresponding to V-groove designs.

For a given normalizing temperature, the YS and UTS decreased with increase in tempering temperature. For V-groove design and fixed normalizing temperature of 1150°C, the maximum UTS and YS were measured to be 730 MPa and 570 MPa respectively for tempering temperature of 730°C, while minimum UTS and YS were measured to be 660 MPa and 520 MPa respectively for tempering temperature of 800°C. For V-groove design, the rate of decrease in UTS was found to be lower up to tempering temperature of 760°C and beyond that, a

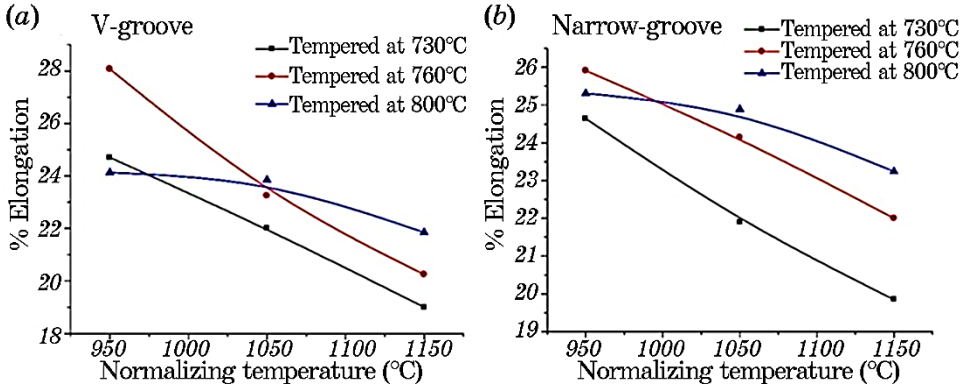

Fig. 16. Variation in % elongation (*a*) V-groove and (*b*) narrow-groove design.

drastic decrease was noticed in the UTS value. For narrow-groove design, a near uniform decreasing trend was observed for given tempering temperature range. The variation in YS and UTS value of P92 steel weldments for different PWNT conditions were strongly affected by the solid solution hardening and precipitate hardening. The coarse precipitates at higher tempering temperature were also responsible for the strength and hardness degradation. The coarse precipitates have poor tendency to act as the dislocation barrier resulting in poor strength and hardness. The increase in tempering temperature led to consumption of C and N from the matrix for higher carbide and carbonitrides precipitation. The reduction of C and N from the matrix resulted in poor solid solution hardening. The formation of precipitate might lead to precipitation hardening but the reduction in solid solution hardening dominates over the increase in precipitate hardening. This resulted in a reduction in strength value of P92 steel at higher tempering temperature. A good agreement was also observed in hardness and strength relationship.

Figures 16, *a*, *b* show the variation [in %] elongation for transverse tensile tested weld specimens in different normalizing and tempering temperature range. The percentage elongation increased with increase in tempering temperature for normalizing temperature range of 1050–1150°C. For V-groove weld design, maximum percentage elongation was measured to be 24.7% for sample normalized at 950°C and tempered at 730°C, while a minimum of 24.13% was for sample tempered at 800°C for same normalizing temperature. The similar pattern of percentage elongation was also measured for narrow-groove design as shown in Fig. 16, *b*. The percentage elongation decreased with increase in normalizing temperature. For tempering temperature of 730°C and normalizing temperature of 1150°C, the percentage elongation was observed to be less than 20% for both the groove designs.

4. CONCLUSIONS

1. The normalizing and tempering treatment, recovery processes leads to the refinement of grain structure. This resulted in higher Charpy toughness value in weld zone than as-received P92 steel.
2. The normalizing and tempering treatment of P92 weldments produced uniformed hardness measured in weld zone and the fine-grained heat affected zone was found to be very much similar to that recorded in as-received P92 steel.
3. The ultimate tensile strength and yield strength value of V-groove weld design were measured to be higher than narrow-groove design while Charpy toughness value of narrow-groove weld design was measured to be superior to V-groove weld design.
4. The final fracture zone of tensile fracture surface revealed the mixed mode of failure for all normalizing and tempering action.
5. The normalizing at 1050°C and 760°C is recommended for P92 weldments for the optimum combination of strength and ductility.

REFERENCES

1. S. L. Mannan, S. C. Chetal, B. Raj, and S. B. Bhoje, *Trans. Indian Inst. Met.*, **35**: 1 (2003).
2. C. Pandey, M. M. Mahapatra, P. Kumar, and N. Saini, *J. Nucl. Mater.*, **498**: 176 (2018).
3. K. L. Murty and I. Charit, *J. Nucl. Mater.*, **383**: 189 (2008).
4. M. Marietta and E. Systems, Ornl/tm—9045 de85 012618 (1984).
5. C. Pandey and M. M. Mahapatra, *J. Mater. Eng. Perform.*, **25**: 2761 (2016).
6. M. E. Abd El-Azim, O. E. El-Desoky, H. Ruoff, F. Kauffmann, and E. Roos, *Mater. Sci. Technol.*, **29**: 1027 (2013).
7. K. Laha, K. S. Chandravathi, P. Parameswaran, K. B. S. Rao, and S. L. Mannan, *Metall. Mater. Trans. A*, **38**: 58 (2007).
8. K. Maruyama, K. Sawada, and J. Koike, *ISIJ Int.*, **41**: 641 (2001).
9. H. K. Danielsen and J. Hald, *Comput. Coupling Phase Diagrams Thermochem.*, **31**: 505 (2007).
10. H. K. Danielsen and J. Hald, *Mater. Sci. Eng. A*, **505**: 169 (2009).
11. M. Abd El-Rahman Abd El-Salam, I. El-Mahallawi, and M. R. El-Koussy, *Int. Heat Treat. Surf. Eng.*, **7**: 23 (2013).
12. V. L. Manugula, K. V. Rajulapati, G. M. Reddy, and K. B. S. Rao, *Mater. Sci. Eng. A*, **698**: 36 (2017).
13. S. K. Albert, M. Matsui, T. Watanabe, H. Hongo, K. Kubo, and M. Tabuchi, *Int. J. Press. Vessel. Pip.*, **80**: 405 (2003).
14. K. Sawada, M. Bauer, F. Kauffmann, P. Mayr, and A. Klenk, *Mater. Sci. Eng. A*, **527**: 1417 (2010).
15. J. A. Francis, W. Mazur, and H. K. D. H. Bhadeshia, *ISIJ Int.*, **44**: 1966 (2004).
16. D. Dean and M. Hidekazu, *Comput. Mater. Sci.*, **37**: 209 (2006).
17. F. William and Jr. Newell, *Weld. J.*, **89**: 33 (2010).

18. M. L. Santella, R. W. Swindeman, R. W. Reed, and J. M. Tanzosh, *EPRI Conf. 9Cr Mater. Fabr. Join. Technol.* (2001).
19. ASTM A370–14, *Standard Test Methods and Definitions for Mechanical Testing of Steel Products* (2014).
20. ASTM E8/E8M–13a, *Standard Test Methods for Tension Testing of Metallic Materials* (2009).
21. D. R. Barbadikar, G. S. Deshmukh, L. Maddi, K. Laha, P. Parameswaran, A. R. Ballal, D. R. Peshwe, R. K. Paretkar, M. Nandagopal, and M. D. Mathew, *Int. J. Press. Vessel. Pip.*, **132–133**: 97–105 (2015).